



Technische Universität München
Department of Electrical Engineering and Information Technology
Bio-Inspired Information Processing

Bachelor's Thesis

Investigation of Cortical Responses to Modulated Noise Stimuli Using fNIRS

Pei-Yi Lin

Date of Submission:
August 29, 2022

Supervisors:
Prof. Dr.-Ing. Werner Hemmert
Dr. Ali Saeedi
M.Sc. Carmen Marie Castañeda González

Abstract

Write your abstract here or use \input{} command.

Acknowledgments

Thanks people!

Contents

1	Introduction	1
1.1	Motivation	1
1.2	Technical Background	2
2	Related Work	4
3	Methods	5
3.1	Study Participants	5
3.2	Probe Design	5
3.3	Acoustic Stimulation during fNIRS Experiment	8
3.4	fNIRS Setup	9
3.5	Data preprocessed	10
4	Results	12
4.1	Waveform Morphology	12
4.2	Regional of Interest	16
5	Discussion	18
6	Future prospectives	19
List of Figures		20
List of Tables		21
References		23

Contents

Chapter 1

Introduction

1.1 Motivation

This research is aimed for better understanding of the brain activities when the subjects are exposed to different audio stimuli with the help of fNIRS measurement.

In the field of neuro-imaging, although fMRI is widely used and provides excellent (spatial) resolution, it still has many limitations, especially when it comes to hearing research. First of all, MRI rooms are noisy, which makes it difficult to control the audio stimulation desired due to inevitable environmental noises. In addition, fMRI scans are done in a magnetic field. It has not yet been proved that pregnant women and infants can be safely exposed to an external magnetic field in the MRI room. For people with hearing disabilities, more specifically cochlear implant patients, going into a MRI room would not be ideal, either. Although there are already cochlear implants that can be worn to a magnetic field, it is still generally not suggested to wear a piece of metal in a MRI room.

fNIRS, short for functional near-infrared spectroscopy. With fNIRS, we can measure brain activity by using near-infrared light to estimate cortical hemodynamic activity which occur in response to neural activity. It is non-invasive and risk-free. The fNIRS device is portable and works silently. With the cap secured on the head, it is also more resilient to motion artifacts. All these makes it ideal for hearing researches. However, it is not yet commonly used in clinical diagnostics due to the lack of understanding of the expected brain activities measured with fNIRS. Therefore, in this research, we'd like to perform some fNIRS measurement and analyse the fNIRS data under different experiment conditions.

If fNIRS can provide more meaningful data and be more commonly used

Introduction

in early clinical diagnosis, we may find hearing abnormality of patients earlier. This is especially important for infants or children. As language development happens in the early stages of one's life, the sooner we find the hearing abnormality and fix it, the better. After a child turns 8, it is practically not possible for him to understand human speech even with perfect hearing. I personally find hearing research a meaningful topic. For one, speech is the primary and direct way of human communication. We express ourselves and perceive other people's opinion via speech. For the other, music has always been an important part of my life for me personally. Without the ability to hear and listen, neither speech nor music will be possible to be perceived. Therefore, I want to help other people with hearing disabilities get better diagnosis and treatment. fNIRS is of great potential to help solve the issue.

1.2 Technical Background

Hemoglobin, the protein from inside red blood cells, transports oxygen molecules throughout the body. Higher hemoglobin levels and red blood cell transfusion are associated with higher cerebral oxygen delivery. Different concentration levels of hemoglobin results in a spectral change. The biological tissue has a relatively good transparency for light in the near-infrared region (700-1300nm) [Jöbsis, 1977]. Therefore, it's possible to transmit sufficient photons *in situ* monitoring.

The technique of NIRS relies on the Beer-Lambert law, which is given by:

$$OD_\lambda = \log\left(\frac{I_0}{I}\right) = \epsilon_\lambda \cdot c \cdot L$$

OD_λ : a dimensionless factor known as the optical density of the medium.

I_0 : the incident radiation.

I : the transmitted radiation.

ϵ_λ : the molar absorptivity ($mM^{-1} \cdot cm^{-1}$) of the chromophore.

c : the concentration (mM) of the chromophore.

L : length of light path.

The Beer-Lambert law was intended for use in a clear, non-scattering medium. When the law is applied to a scattering medium, e.g. brain tissue, a correction factor should be applied. The factor, called "differential path-length factor (DPF)" accounts for the increase in optical path length due to scattering in the tissue. The modified Beer-Lambert law is given by:

$$OD_\lambda = \epsilon_\lambda \cdot c \cdot L \cdot B + OD_{R,L}$$

1.2 Technical Background

where $OD_{R,L}$ represents the oxygen-independent light absorption due to scattering in the tissue, and B is the mean pathlength traveled by the detected photons. In our case, i.e. CW-NIRS, this mean pathlength is not known. In a highly scattering medium, the pathlength of trajectories is longer than the source-detector separation. Nevertheless, one may still estimate the pathlength within the whole sampling region by multiplying the source-detector distance with a DPF. Assuming $OD_{R,L}$ is constant during a measurement, we may rewrite the previous equation in terms of changes in optical density and changes in concentration as follows:

$$\Delta c = \frac{\Delta OD_\lambda}{\epsilon_\lambda \cdot L \cdot B}$$

The validity of the above equation depends on how much B varies. [Delpy et al., 1988] investigated this question and gave a relation between the DPF and the head diameter. Nonetheless, newer research also provides different ways to estimate the DPF. In the scope of this project, the DPF was calculated from a function of wavelengths and age of the participant [Duncan et al., 1996].

Chapter 2

Related Work

Chapter 3

Methods

3.1 Study Participants

We measured 8 normal hearing people. Participant 8 was given silent stimuli as a comparison. The detailed information about the subjects are listed in the table.

Participant	Gender	Handedness	Race	Hair color	Age
1 chang	F	right-handed	east asian	dark	22 yr
2 gleb	M	right-handed	caucasian	blond	18
3 jonas	M	left-handed	caucasian	brunet	21
4 lin	F	right-handed	east asian	dark	21
5 lukas	M	right-handed	caucasian	blond	26
6 shelia	F	right-handed	southeast asian	dark	22
7 liao.	M	right-handed	east asian	dark	22
8 lukas	M	right-handed	caucasian	blond	22

Table 3.1: Study Participants.

3.2 Probe Design

The probes were first designed in AtlasViewer [pic] [Aasted et al., 2015] and the SD GUI interface. I tried to replicate the probe design as close as possible to the research from Weder et al. However, several modifications need to be made due to device limitations.

First of all, the paper only provided a rough 2D-sketch of their probe design. [see pic] The channels were not described in detail. Though there are

Methods

different ways to define the channels, we believe it shouldn't matter as long as the mid-points of the channel correspond to that of the previous research.

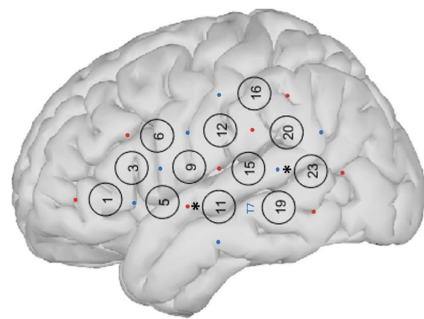
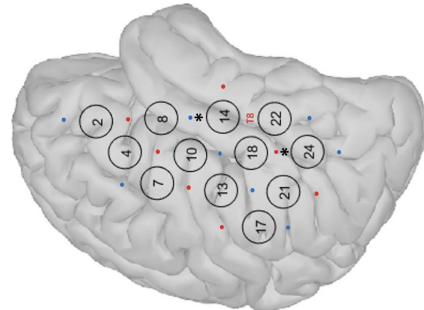


Figure 3.1: Probe design from Weder et al.

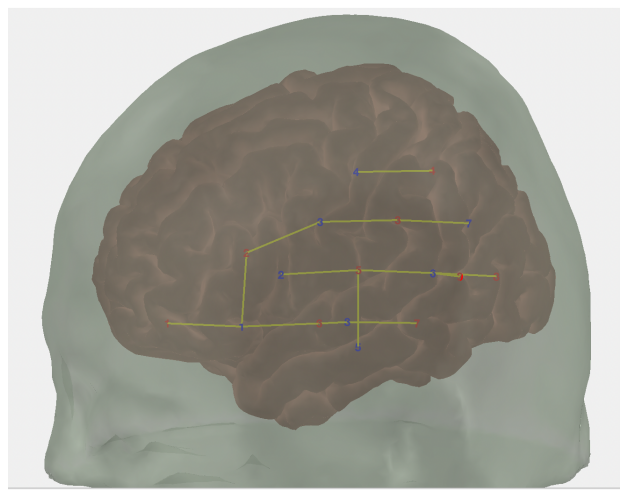


Figure 3.2: Probe design in this research. Shown in AtlasViewer. The red numbers represent the light sources and the blue numbers represent the detector. Channels are shown in yellow lines.

3.2 Probe Design

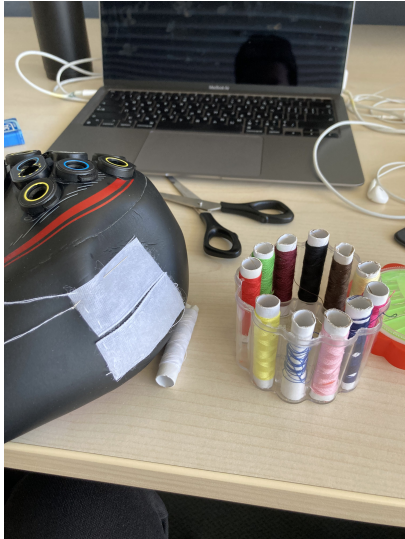


Figure 3.4: Manufacturing process of the cap



Figure 3.5: Finished cap on dummy

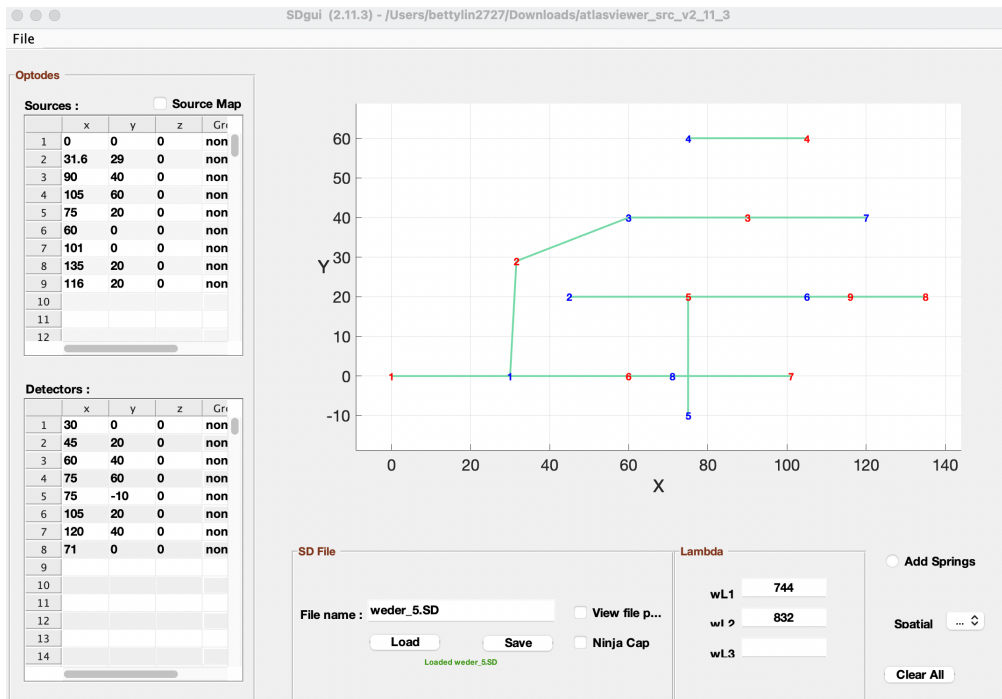


Figure 3.3: SDgui interface and optode coordinates.

Due to device limitations, we only measured one side of the brain. According to previous research [Frost et al., 1999], language processing has

Methods

been predominantly associated to cortical activity in the left hemisphere. As a result, we've decided to focus on the left hemisphere.

The fNIRS device we use also has limited number of sources and detectors. If we'd like to keep the original design, we'd need 9 sources and 9 detectors. However, the device we are using has only 10 sources and 8 detectors. Hence, we shifted one channel around T7 a little bit to the left, so that one less detector is needed. At the end, there were 12 long channels and 2 short channels in our setup.

For the software usage, an .xml file is required. In the .xml file, the sources, detectors, and channels are defined. Different optode templates for different probe design can be stored in one single .xml file. The physical cap was self-made from a swimming cap. With the help of a dummy head model, correct positions of the optodes were marked and holes were drilled accordingly. The mounts were put on the cap on the holes. In order to ensure the correct channels length to be fixed exactly at 30 mm, plastic holders were also placed on the long channels. As for the short channels, the package comes with mounts for short channels. Thus, no plastic holders were needed in the case. The short channels were 11 mm long. The self-made cap turned out to work out well. The contacts between the scalp and the optodes were good thanks to the elastic characteristic of the material.

3.3 Acoustic Stimulation during fNIRS Experiment

Auditory stimuli were delivered binaurally via an audio metric headphone (Sennheiser HD 650). Stimuli consisted of 20-s chunks of the ICRA noise [Dreschler et al., 2001].

To begin with, ICRA noise was developed to be used as background noise in clinical tests of hearing aids and possibly for measuring characteristics of non-linear instruments. The signals are based on live English speech from the EUROM database [Chan et al., 1995] in which a female speaker is explaining about the system of arithmetical notation. The speech signals were sampled with a sampling rate of 44.1 kHz. By composing the speech signals with well defined spectral and temporal characteristics, the modified signals have long-term spectrums but are completely unintelligible.

We chose to use ICRA noise as stimuli based on several reasons. For one, ICRA noise is broadband amplitude-modulated signal. By selecting a broadband stimulus, broad cortical auditory areas are activated more strongly compared with simple static stimulus. The bandwidth of auditory stimuli is

3.4 fNIRS Setup

positively correlated with the mean percentage signal change and spread of cortical activation [Hall et al., 2001]. Previous fMRI study also manifested that more complex auditory stimuli elicit greater response in most parts of the auditory cortes [Belin et al., 2002]. For the other, ICRA noise is a well-known and accessible stimulus. It is also considered as an international de facto standard for hearing research. In this way, our results can be comparable with other researches.

As for choosing different sound level pressure, we picked 40 dB, 65 dB, 90 dB, and silent stimulus, i.e. 0 dB. Calibrations were performed using an oscilloscope, a G.R.A.S. Power Module Type 12AK, and an artificial ear (G.R.A.S. 43AA). The artificial ear transform the SPLs (sound pressure levels) into electrical signals, i.e. voltages that can be measured by the oscilloscope. According to the instruction manual of the G.R.A.S. artificial ear, the measured level is 11.19 [$\frac{mV}{Pa}$] and we know the SPL in dB is defined as

$$SPL[dB] = 20 \cdot \log \frac{P}{P_0}, \text{ where } P_0 \text{ is } 20\mu\text{Pa}$$

Hence, the relation between SPL and measured voltage should be.

$$V = 20\mu\text{Pa} \cdot 10^{\frac{SPL}{20}} \cdot 10^{\frac{Gain}{20}} \cdot 11.19 \frac{mV}{Pa}$$

The headphone with the artificial ear were setup together in the sound booth to ensure minimal environmental noise. The output voltages were measured with the oscilloscope. This way, the corresponding amplitude inputs for later MATLAB scripts for the desire SPLs can be determined.

MATLAB and Oxysoft were used during the measurement. In MATLAB, a chunk in the ICRA audio files was selected. It was multiplied with different amplitude levels for 4 SPLs and ramped by a 10-ms Hanning window. In each epoch, all four stimuli (0dB, 40 dB, 65 dB, and 90 dB) were played randomly once. After each stimulus, there was a 25-sec silence rest to wait for the hemodynamic response. For each participant, 8 epochs were conducted. The stimuli were marked with Labstreaminglayer to note which SPL it was. This Labstreaminglayer also acted as an interface between MATLAB and Oxysoft, so that Oxysoft could mark the time for each stimulus in the measurement data correctly in real time.

3.4 fNIRS Setup

The Brite23 was used in this research. It is light weight, has 10 sources and 8 detectors and can support up to 23 channels. The Brite23 fNIRS

Methods

device was connected via bluetooth to the PC and the Oxysoft software. For each measurement, the DPF is calculated depends on the age of the participant. The sampling rate was fixed at 50 Hz, for enough resolution but not unnecessary too large in terms of data size.

After the setting in the Oxysoft software was done, the participant would be asked to put on the self-made cap. On each optode position, the hair would be put aside gently with a Q-tip to ensure better contact between the optodes and the scalp. Then, the participants would be asked to put on the headphone and go into the sound booth.

3.5 Data preprocesion

Data preprocessing and analysis was executed in MATLAB (Mathworks, USA) and the Homer3 toolbox. The following steps were executed.

First, the hemodynamic response was extracted with the Homer3 toolbox. Raw data were converted into optical densities. Motion artifacts were removed by using wavelet transformation of the data. The Homer3 toolbox bandpass filter (0.01 and 0.5 Hz) reduced drift, broadband noise, heartbeat, and respiration artifacts. Concentration if oxygenated and deoxygenated hemoglobin were estimated by applying the modified Beer-Lambert Law [Delpy et al., 1988]. Strictly speaking, the DPF should be experimentally obtained with FD-NIRS or TD-NIRS. However, due to device limitation, it is not possible in this project. Hence, in our research, the DPF was determined by wavelengths of the fNIRS device and age of the participant. [Duncan et al., 1996]. With the given literature, the DPF for two wavelength is calculated with the formulas:

$$DPF_{744} = 5.11 + 0.106 \cdot Age[yr]^{0.723}$$

$$DPF_{852} = 4.67 + 0.062 \cdot Age[yr]^{0.819}$$

The paper has only given the formulas for four wavelengths. Although we used different wavelengths $\lambda = 757[nm]$ and $\lambda = 843[nm]$. We are convinced that the calculated DPF would be very close to the ones calculated with the above two equations.

It is important to note that the noise due to motion artifacts, drift, broadband noise, heartbeat, and respiration artifacts need to be processed before the concentration was estimated, according to the previous research [Huppert et al., 2009].

Later on, the extracerebral component in long channels should be reduced by using measurements from the short channels as follows: the first

3.5 Data precession

principal components from the two short channels were estimated and then multiplied by its coefficient from the GLM (general linear model). However, this is not done in the scope of this research. The coefficient from the GLM were very small. They were of the magnitudes 10^{-16} , whereas the hemodynamic response in the long channels were of the magnitudes 10^{-5} . Hence, we concluded the extracerebral components in our case can be negligible.

Channels with unusable data were excluded here for further analysis. The scalp coupling index (SCI) is a common measure in this case. It is originally described in [Pollonini et al., 2013]. In short, the SCI estimates the correlation between the two wavelength channels in the cardiac band as the following:

First, the signal is bandpass-filtered to keep only the cardiac band. In our case, a wide band of [0.5 - 2.5] Hz was chosen. Then, amplitude normalization is performed, and the SCI computation is defined as the absolute cross-correlation value at 0-time lag.

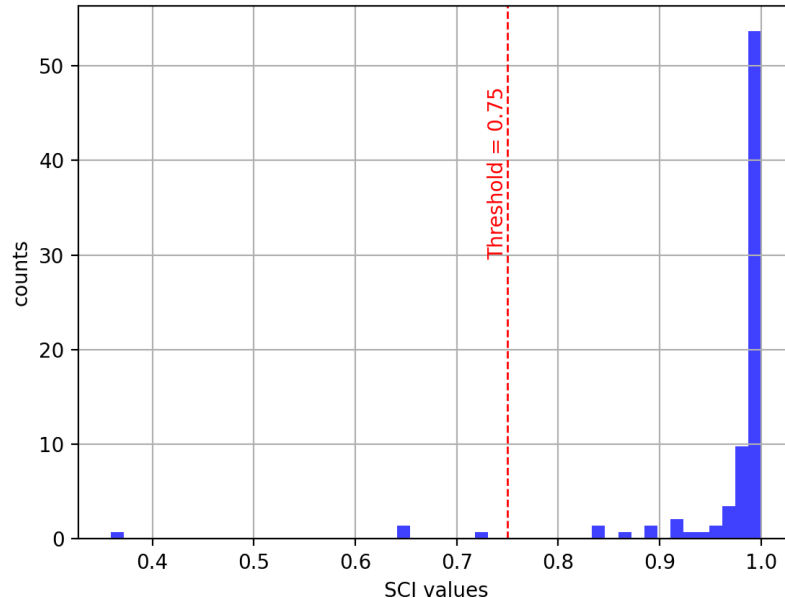


Figure 3.6: Distribution of SCI values.

In this project, only 4 channels failed to reach the threshold = 0.75. In other words, of all the measurements (14 channels per participant, 8 participants in total.) That means over 96% of the measurements passed the SCI threshold.

Chapter 4

Results

4.1 Waveform Morphology

From our measurements, the results varies a lot individually. Hence, grand average and further statistical analysis won't be well-applicable. In this section, waveform morphology of the 14-channel measurements for some of the participants are shown and described.

First of all, our channels with the optode template are defined as this figure. [picture to be added]

In the following figures. Measurements in all channels are plotted in the same scale except for the two short channels marked in thicker outlines. Channels with invalid SCI won't be taken into consideration, and hence are not shown.

4.1 Waveform Morphology

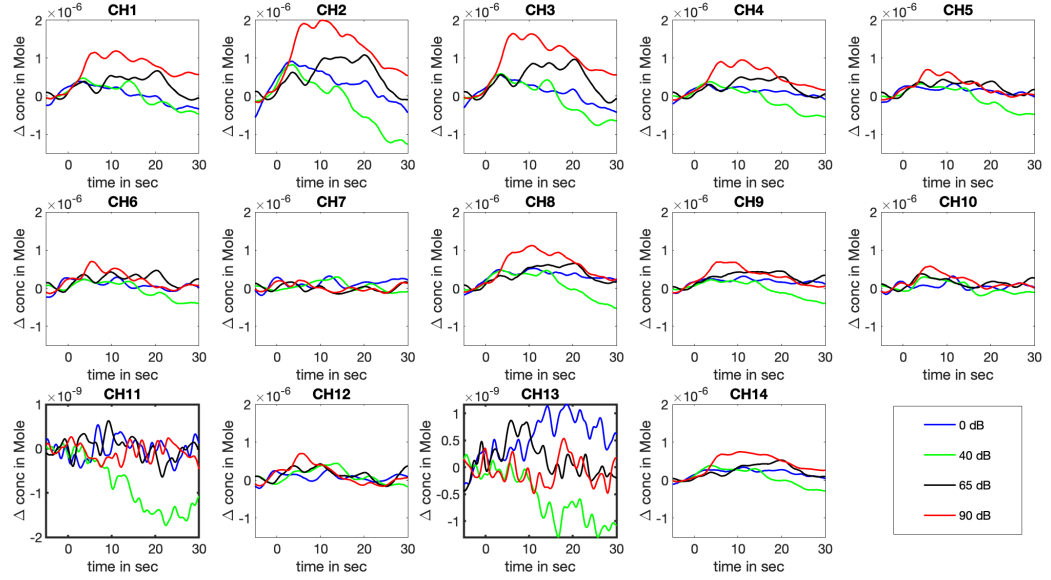


Figure 4.1: Measurement from participant 3.

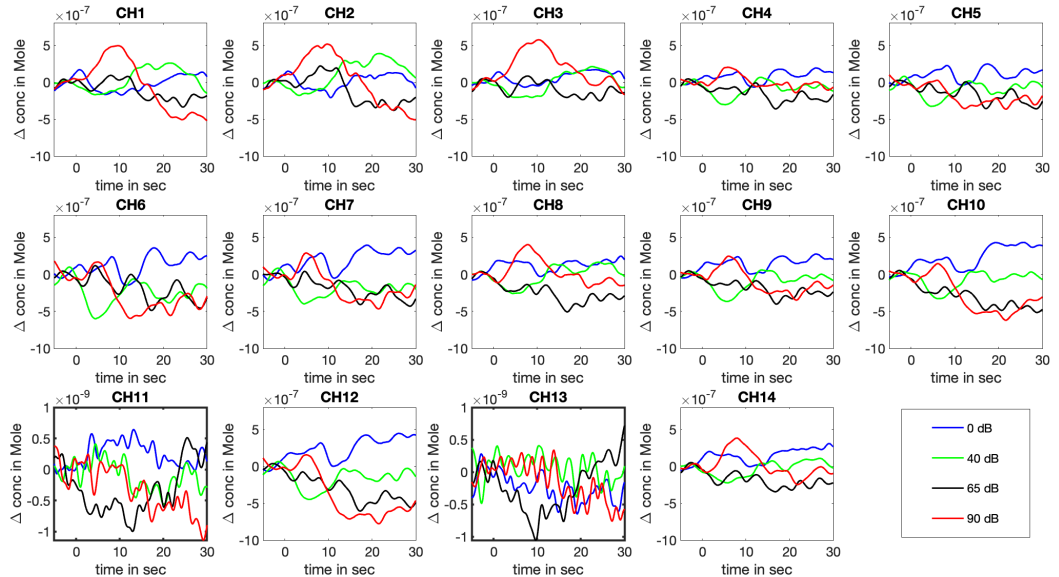


Figure 4.2: Measurement from participant 5.

Results

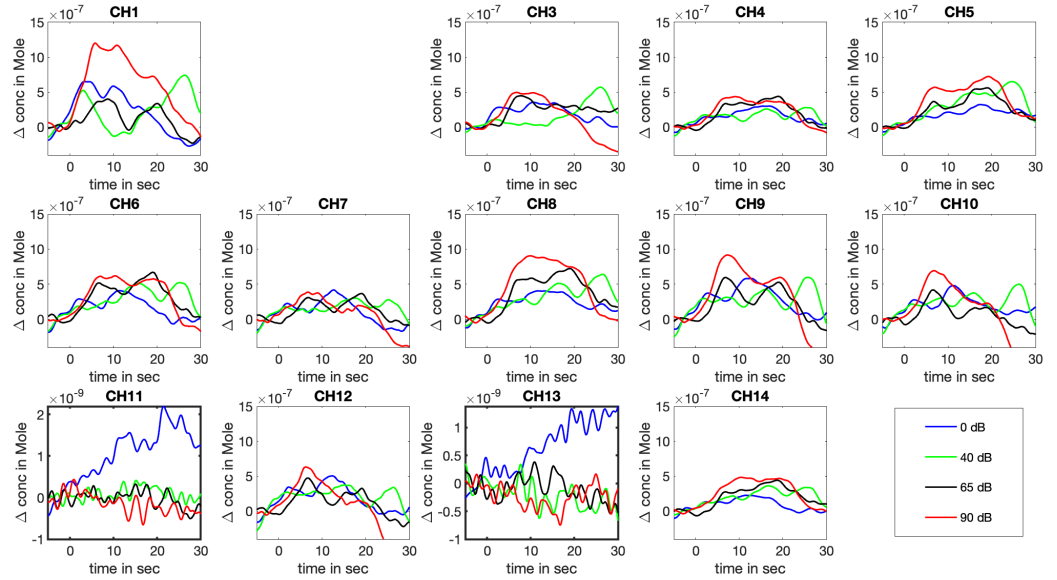


Figure 4.3: Measurement from participant 7.

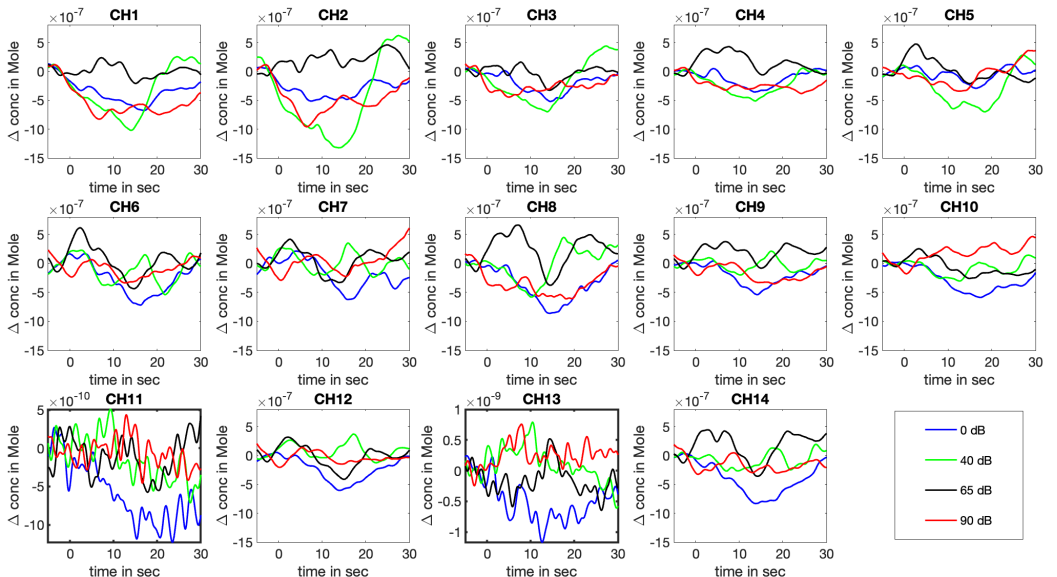


Figure 4.4: Measurement from participant 8. Silent comparison

4.1 Waveform Morphology

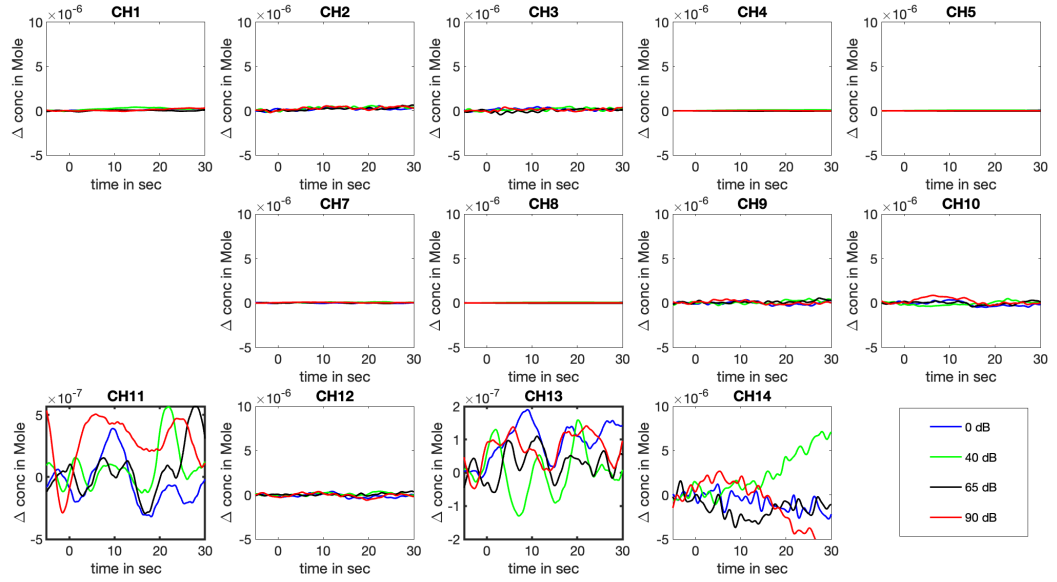


Figure 4.5: Measurement from participant 4.

Results

4.2 Regional of Interest

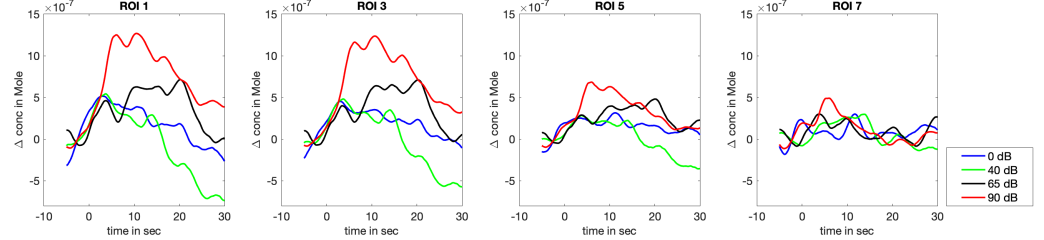


Figure 4.6: Measurement from participant 3.

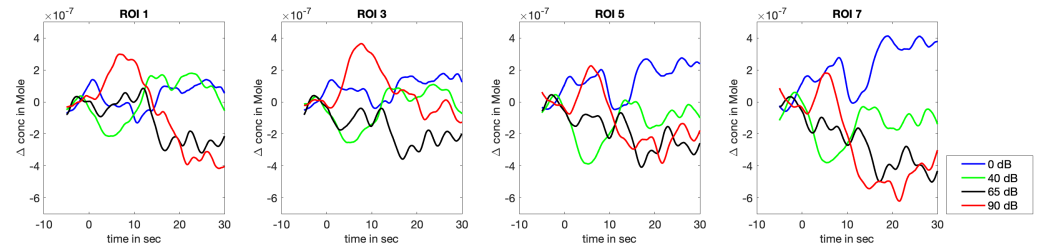


Figure 4.7: Measurement from participant 4.

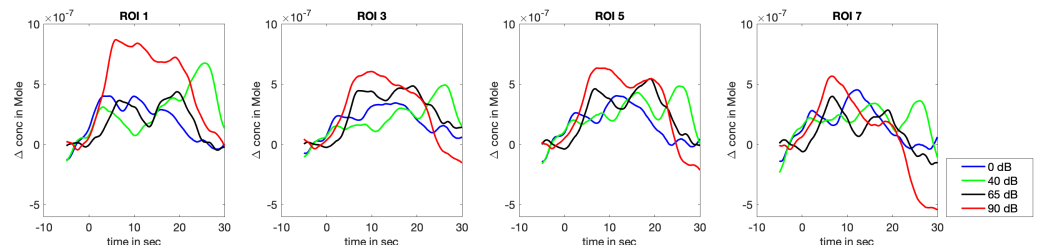


Figure 4.8: Measurement from participant 7.

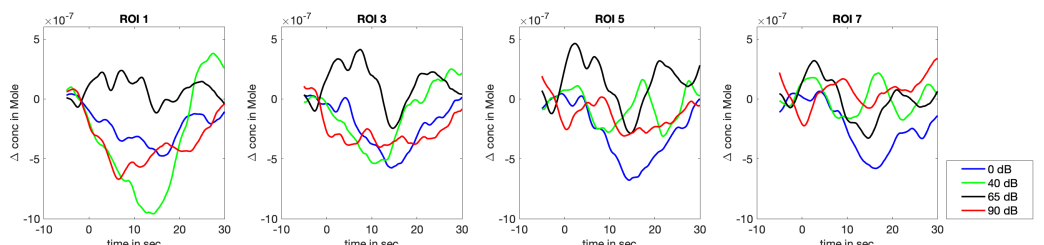


Figure 4.9: Measurement from participant 8. Silent comparision.

4.2 Regional of Interest

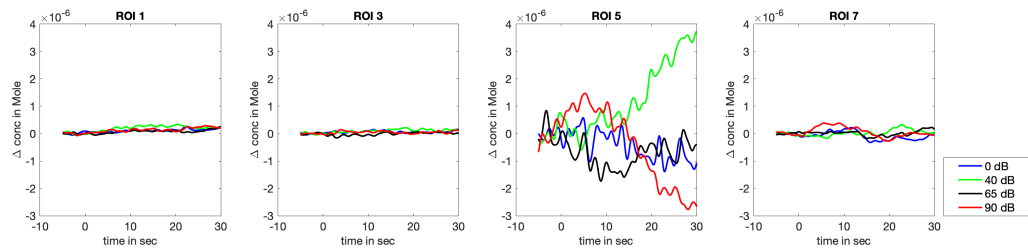


Figure 4.10: Measurement from participant 4.

Chapter 5

Discussion

Chapter 6

Future prospectives

List of Figures

3.1	Probe design from Weder et al.	6
3.2	Probe design in this research. Shown in AtlasViewer. The red numbers represent the light sources and the blue numbers represent the detector. Channels are shown in yellow lines.	6
3.4	Manufacturing process of the cap	7
3.5	Finished cap on dummy	7
3.3	SDgui interface and optode coordinates.	7
3.6	Distribution of SCI values.	11
4.1	Measurement from participant 3.	13
4.2	Measurement from participant 5.	13
4.3	Measurement from participant 7.	14
4.4	Measurement from participant 8. Silent comparison	14
4.5	Measurement from participant 4.	15
4.6	Measurement from participant 3.	16
4.7	Measurement from participant 4.	16
4.8	Measurement from participant 7.	16
4.9	Measurement from participant 8. Silent comparision.	16
4.10	Measurement from participant 4.	17

List of Tables

3.1 Study Participants.	5
---------------------------------	---

Bibliography

- [Aasted et al., 2015] Aasted, C. M., Yücel, M. A., Cooper, R. J., Dubb, J., Tsuzuki, D., Becerra, L., Petkov, M. P., Borsook, D., Dan, I., and Boas, D. A. (2015). Anatomical guidance for functional near-infrared spectroscopy: AtlasViewer tutorial. *Neurophotonics*, 2(2):020801.
- [Belin et al., 2002] Belin, P., Zatorre, R., and Ahad, P. (2002). Human temporal-lobe response to vocal sounds. *Brain research. Cognitive brain research*, 13:17–26.
- [Chan et al., 1995] Chan, D., Fourcin, A., Gibbon, D., Granstrom, B., Hucvale, M., George, K., Kvale, K., Lamel, L., Lindberg, B., Moreno, A., Mouropoulos, J., and Senia, F. (1995). Eurom - a spoken language resource for the eu. *Proc. Eurospeech*, 1.
- [Delpy et al., 1988] Delpy, D. T., Cope, M., van der Zee, P., Arridge, S., Wray, S., and Wyatt, J. (1988). Estimation of optical pathlength through tissue from direct time of flight measurement. *Physics in Medicine and Biology*, 33(12):1433–1442.
- [Dreschler et al., 2001] Dreschler, W., Herschuure, H., Ludvigsen, C., and Westermann, S. (2001). Icra noises: Artificial noise signals with speech-like spectral and temporal properties for hearing aid assessment. *Audiology*, 40:148–157.
- [Duncan et al., 1996] Duncan, A., Meek, J., Clemence, M., Elwell, C. E., Fallon, P., Tyszcuk, L., Cope, M., and Delpy, D. T. (1996). Measurement of cranial optical path length as a function of age using phase resolved near infrared spectroscopy. *Pediatric Research*, 39:889–894.
- [Frost et al., 1999] Frost, J. A., Binder, J. R., Springer, J. A., Hammeken, T. A., Bellgowan, P. S., Rao, S. M., and Cox, R. W. (1999). Language processing is strongly left lateralized in both sexes. evidence from functional MRI. *Brain*, 122 (Pt 2):199–208.

Bibliography

- [Hall et al., 2001] Hall, D., Haggard, M., Summerfield, A., Akeroyd, M., Palmer, A., and Bowtell, R. (2001). Functional magnetic resonance imaging measurements of sound-level encoding in the absence of background scanner noise. *The Journal of the Acoustical Society of America*, 109:1559–70.
- [Huppert et al., 2009] Huppert, T. J., Diamond, S. G., Franceschini, M. A., and Boas, D. A. (2009). Homer: a review of time-series analysis methods for near-infrared spectroscopy of the brain. *Appl. Opt.*, 48(10):D280–D298.
- [Jöbsis, 1977] Jöbsis, F. F. (1977). Noninvasive, infrared monitoring of cerebral and myocardial oxygen sufficiency and circulatory parameters. *Science*, 198(4323):1264–1267.
- [Pollonini et al., 2013] Pollonini, L., Olds, C., Abaya, H., Bortfeld, H., Beauchamp, M., and Oghalai, J. (2013). Auditory cortex activation to natural speech and simulated cochlear implant speech measured with functional near-infrared spectroscopy. *Hearing research*, 309.

Bibliography

Erklärung der Selbstständigkeit

Hiermit versichere ich, die vorliegende Arbeit selbstständig verfasst und keine anderen als die angegebenen Quellen und Hilfsmittel benutzt sowie die Zitate deutlich kenntlich gemacht zu haben.

.....
Ort, Datum

Pei-Yi Lin